

A BRIEF REVIEW ON IMMOBILIZATION OF GOLD NANOPARTICLES ON INORGANIC SURFACES AND SUCCESSIVE IONIC LAYER DEPOSITION

L.B. Gulina, A.A. Pchelkina, K.G. Nikolaev, D.V. Navolotskaya, S.S. Ermakov and V.P. Tolstoy

Institute of Chemistry, St. Petersburg State University, Universitetsky pr. 26, 198504 St. Petersburg, Russia

Received: May 14, 2015

Abstract. In this review, peculiarities of the Gold nanoparticles synthesis on the solid support are discussed. This article focuses on the recent developments in various methods for immobilization of gold nanoparticles on solid surface. Particular attention is given to the synthesis of nanoparticles by Layer-by-Layer method and on the advances in the Successive Ionic Layer Deposition (SILD) methodology. The present review summarizes SILD work in this field to date and contributes a new experimental data for application SILD method in field of electrochemical sensor design.

As an example the conditions of synthesis of gold nanoparticles on the surface of indium-tin oxide (ITO) electrode are described in this article. It has been shown that the size of synthesized nanostructures can be controlled by formation of intermediated layer. It was found that preliminary SILD synthesis of $Au_xSnO_2 \cdot nH_2O$ nanolayer on the ITO surface leads to significant changes in the morphology of subsequently synthesized gold nanoparticles. In this case the same number of cycles provides the formation of significantly smaller (10-20 nm) nanoparticles and greater surface coverage density. Electrodes obtained by this technique demonstrate lower oxidation and reduction potentials of gold as well as higher currents of these reactions.

1. INTRODUCTION

The Gold nanoparticles sols had been known in the 17th century. Faraday was the first to present in 1857 a scientific paper on their properties and preparation [1]. At now, the Gold nanoparticles (AuNPs) represent one of the most remarkable areas of modern nanoscience and nanotechnology. The unique optical, catalytic, bio-functional properties of gold colloids have attracted substantial interest in recent years. Gold nanoparticles are one of the most promising materials as catalyst [2], sensor [3], biosensor [4], contrast agents [5], drug delivery agent [6,7], smart nanomaterial [8,9] and other. The properties and applications of AuNPs strongly depend upon their size and shape. Many methods have been

developed to prepare of gold nanoparticles, varying by shape and size [10-12]. For example, gold nanoparticles can be synthesized using various chemical and physical deposition techniques, such as simple chemical reduction in solution [13], synthesis in hydrothermal conditions [14], two-phase synthesis [15], sputtering [16], laser ablation [17], evaporation [18], plasma synthesis [19], and other. Many of chemical and physical methods, applicable for synthesis and deposition of gold nanoparticles (clusters) with average diameters from 5 to 150 nm, were discussed in recent reviews [3,12,20].

The main aim of this paper is to give a brief overview of recent experiments on immobilization of Gold nanoparticles on the various inorganic solid supports.

Corresponding author: L.B. Gulina, e-mail: l.gulina@spbu.ru

2. APPROACHES TO GOLD NANOPARTICLES IMMOBILIZATION

In this context, an increasing attention is paid to development of new facile techniques of preparing of gold nanoparticles immobilized on the surface of solid support. AuNPs synthesized on the surface attract attention of many researchers because of their unique properties and opportunities for various applications [21,22]. It is known that gold nanoparticles supported by metal oxides become very catalytically active at certain cluster sizes. In particular, gold nanoparticles deposited on electrode surface have already found applications in chemical sensors, including gas sensors [23] and biosensors [24].

Among the physical methods of synthesis on surface the chemical vapor deposition (CVD) can be used for the AuNPs forming. $\text{HAuCl}_4 \cdot 3\text{H}_2\text{O}$ [25] or $(\text{CH}_3)_3\text{PAuCH}_3$ [26] were used as precursors for the CVD synthesis. The CVD is industrially used technique for nanoparticles deposition on variety substrates. However, the CVD method is expensive and has limitations in the formation of clusters on surfaces. The other physical methods, based on temperature decomposition of precursors often led to changes of the particle sizes. Wet methods have no such limitations and that is why they started attracting greater attention. The AuNPs on the surface of preformed silica microspheres have been obtained by a sonochemistry method [27].

The methods of transfer of nanoparticles from colloidal solution of them are widely used to immobilize gold nanoparticles onto the surface, for example self-assembly or Langmuir-Blodgett method [28]. In this case solutions of colloidal particles with certain size are used as precursors. The most widely used method of chemical synthesis of gold nanoparticles in solution is the Turkevich-Frens method based on the classic citrate reduction of gold (III) derivatives [29]. Another popular method for AuNPs synthesis is Brust-Schiffrin method [15]. The gold precursors are reduced by sodium borohydride (NaBH_4) in an organic solvent using either a two-phase liquid/liquid system or a suitable single-phase solvent. Surface-active additives usually are used to control a particle shape and size in process of the wet synthesis [30,31]. Typical ligand molecules for gold nanoparticles in solution are amines, phosphines, thiolates and other sulfur-containing organic reagents. Among them thiolates are the most investigated ligand molecules. However, it was found that additives used for the AuNPs size

stabilization were the source of sulfur and other impurities. These impurities together with chlorine ions from common precursor HAuCl_4 can be incorporated in the synthesized gold nanoparticles and adversely affect their functional properties.

The deposition-precipitation (DP) method is widely used for preparing of powder catalysts with AuNPs [32]. A typical procedure for this synthesis is as follows. The nominal amount of aqueous solution of HAuCl_4 is added into a solution containing suspended oxide support. Then the NaOH (or NH_4OH) solution is brought to the required pH in suspended solution. After aging the precipitate is recovered, exhaustively washed to remove Cl⁻ ions and reduced to form AuNPs. As result of such treatment it is possible to obtain small gold metal particles with average sizes 1-3 nm on the silica, zirconia, titania, and alumina supports [33-35].

An important rout in the formation of AuNP on the surface was achieved recently with the layer-by-layer (LbL) method [36,37]. In 1966 for the first time Iler reported the formation of layer on the support by alternating deposition of positively and negatively charged colloid particles [38]. A similar technique could be used not only to colloid particles. The LbL method based on fabrication of nanostructured films through specific interactions of structural units at the support surface [39-41]. LbL theoretical aspects were studied to understanding the driving forces responsible for the formation of layers in recent years. The driving force is based on electrostatic interactions between charge ions and particles, covalent bonding, hydrophobic interactions, coordination bonding, Van der Waals forces and hydrogen bonding [42].

Many works have been published about the synthesis of nanogold using of the LbL method for multiplex applications involving sensors and biosensors [43,44]. LbL growth of multilayers on surfaces, where AuNPs are included in layer composition, has been demonstrated by several groups [45-47]. Nanolayers with AuNPs obtained by LbL method usually contain polyelectrolyte molecules which sometimes serve as a «sticking» layer between the substrate and nanoparticles, and other substances, including carbon nanotubes, graphene, chitosan, polyoxometalate and other [48-52]. Usually the colloidal solutions of AuNPs, stabilized by surfactant molecules are used as precursors in synthesis of the multicomponent layer by LbL methodology.

One should also take into account that many of indicated above additives such as thiols and others stabilizers are toxic. Another problem with AuNPs immobilization on the surface is the removal of or-

ganic molecules of surfactants from the layer of gold nanoparticles. Generally a heat treatment is used to remove indicated above additives, therefore an agglomeration of nanoparticles takes place at times. As a result, there are difficulties with controlling both the cluster size, and the adhesion of coatings formed.

3. SUCCESSIVE IONIC LAYER DEPOSITION TECHNOLOGY.

The Successive Ionic Layer Deposition (SILD) method [53-56] is one of LbL technologies. The synthesis by SILD is performed without the use of polyelectrolyte solutions and in such a way makes it possible to simplify the procedure significantly and get the coating that contain only inorganic compounds, which is important in many cases. SILD technology, described in the present article, also refers to the chemical deposition methods and therefore this technique has all advantages of wet chemical methods designed for AuNPs synthesis. In addition, SILD methodology, because of its specificity, has a distinctive feature – the ability to control the particle size; SILD methodology is a multi-step process, wherein the size control of deposited particles can be achieved by multiple repetitions of chemical treatments. Previously, a series of high-performance gas sensors based on SnO_2 was developed using this method [57-60]. The optimal conditions for the synthesis of $\text{Au}_x\text{SnO}_2 \cdot n\text{H}_2\text{O}$ nanocomposite layer were found in [61]. The gold in the indicated composite is in the metallic state. It is shown that as a result of successive treatments the nanocomposite layer with a Sn/Au ratio varying from 1:1 to 6:1 can be formed on the solid surface. The size of the Au clusters incorporated in the SnO_2 matrix is in the range from 3 to 15 nm. Gas sensing characteristics of SnO_2 films modified by SnO_2 -Au nanocomposites are discussed as well as. In [62] it is shown that surface modification by SnO_2 -Au nanocomposites can be used for improving operating characteristics of conductometric SnO_2 -based gas sensors, namely a conductivity response to such reducing gases as CO and H_2 .

The ability of SILD technology to synthesize AuNPs on the surface of tin (IV) oxide and indium (III) oxide films is discussed in [63]. It is shown that during the treatment of the surface of tin (IV) oxide and indium (III) oxide films by SILD procedures, conditions can be realized under which the size of gold nanoclusters may be controllably varied between 1–3 nm and 50 nm.

Detailed analysis of the results obtained in the field of immobilization AuNPs allowed us to summarize the most important peculiarities of this. Firstly, the traditional approach using a colloidal solution of nanoparticles as reagent leads to formation of AuNPs surrounded by surfactant molecules. It is useful for achievement a required functionality of particles for particular applications, for example in biomedicine. At the same time, contamination of the active surface of the particles is disadvantageous for other applications, such as sensor design. It is important that gold clusters having size in indicated range can be received without using any surfactants by SILD. This means that SILD method can be used for purposes that require the presence of gold nanoclusters with desired size on the inorganic oxide surface, in particular in catalysis and gas sensor applications. Secondly, for activation of the inorganic oxide/Au system it should be annealed at a temperature of 100–200 °C without aggregation of AuNPs. Thirdly, at the same time, the synthesized particles should be uniformly dispersed on surface of oxide support. One should note that the advantages SILD method include precise control of the size of formed AuNPs. Fourthly, the selection of appropriate support oxides is also required to achievement of reactivity of AuNPs [64]. We believe that this problem is of interest, because the peculiarities of AuNP deposition on various inorganic surfaces still present a great challenge.

The second objective of this paper is to investigate the effect of previously synthesized layer on the morphology of gold nanoparticles forming by SILD method.

4. EXPERIMENTAL

4.1. Chemicals and instruments

The morphology of synthesized nanoparticles was studied using the «Zeiss Merlin» scanning electron microscope. UV-vis absorption spectra were obtained using Perkin-Elmer Lambda 9 spectrophotometer. Electrochemical measurements were carried out using «P-30SM» potentiostat-galvanostat (Elins, Russia). Electrochemical cell consisted of a working ITO electrode, silver chloride reference electrode (SCE) and platinum counter electrode. The working electrode was indium-tin oxide layer with 100 nm thickness and 20 Ohms resistance obtained by magnetron dispersion method on a glass surface. H_2SO_4 used for the electrochemical measurements were supplied from Vekton and Aldrich, their purity was $\geq 99.5\%$. NaBH_4 (99%), SnF_2 (99%) received

from Sigma Aldrich, and $\text{HAuCl}_4 \cdot n\text{H}_2\text{O}$ (49.47% of Au) from Aurat Ltd. were used for the SILD synthesis. All solutions were made using deionized water with resistivity not less than $18 \text{ M}\Omega \text{ cm}$ at 298K (D-301 deionizer, Akvilon, Russia).

4.2. SILD synthesis

Immediately before the synthesis of gold nanoparticles the substrate was washed in acetone in ultrasonic bath for removal of contaminants. Then the substrate was kept in hydroalcoholic (1:1) NH_4OH solution (pH 7-8) for 1 hour in order to achieve the wettability of the surface by aqueous solutions. The SILD synthesis of gold nanoparticles on ITO surface was performed by the technique described elsewhere [63]. The substrate was treated many times by means of serial immersion in 0.001 M HAuCl_4 solution and 0.01 M NaBH_4 solution, which acted as a reducing agent. The rinsing of the substrate with deionized water after each step of the treatment was obligatory. Thus, one SILD cycle consisted of the immersion of the substrate into HAuCl_4 solution, rinsing the substrate with water, immersion into NaBH_4 solution and rinsing with water again. The duration of the treatment in solution was 30-60 sec. and the number of synthesis cycles varied from 4 to 12 according to the experimental tasks. Two batches of electrode samples were produced. The first batch consisted of electrodes obtained after 4 – 12 cycles of SILD synthesis of gold nanoparticles on ITO substrate. The samples of this batch were marked as Au(n4), Au(n6), Au(n8), etc., the numeral indicating the number of SILD cycles. The second batch of electrode samples was similar to the first one, but $\text{Au}_x\text{SnO}_2 \cdot n\text{H}_2\text{O}$ layer was synthesized on ITO substrate surface prior to gold nanoparticles synthesis. The layer of $\text{Au}_x\text{SnO}_2 \cdot n\text{H}_2\text{O}$ was obtained by three SILD cycles, 0.01 M SnF_2 solution and 0.001 M HAuCl_4 solution used as reagents [61]. The samples of the second batch were marked as $\text{Au}_x\text{SnO}_2(n3)\text{-Au}(n4)$, $\text{Au}_x\text{SnO}_2(n3)\text{-Au}(n8)$, etc. The numerals also indicate the numbers of SILD cycles used for Au_xSnO_2 and gold nanoparticles synthesis respectively. After the synthesis, the obtained electrodes were kept for 5-10 minutes in deionized water and then they were dried for 30 minutes in a 250°C oven under the air atmosphere.

4.3. Electrochemical measurements

Electrochemical studies of the electrodes with the synthesized layers were carried out using cyclic

voltammetry. The cyclic voltammetric scans started from 0 V to +1.5 V and then back to 0 V vs. SCE at 50 mV/s were obtained in 0.1 M sulfuric acid solution.

5. RESULTS AND DISCUSSION

5.1. SILD synthesis and characterization of the gold nanoparticles

As a result of SILD synthesis on the surface of ITO electrode gold nanoparticles are formed (Fig. 1). Concerning morphology of the ITO electrode it can be concluded that it is formed by crystal with diameters of 20-50 nm (Fig. 1a). Fig. 1b presents a microphotograph of the electrode after 8 SILD cycles. Evenly located nanoparticles with the average diameter of 40-50 nm are observed on the surface. As a result of $\text{Au}_x\text{SnO}_2 \cdot n\text{H}_2\text{O}$ synthesis a nanocomposite layer consisting of amorphous tin oxide and gold nanoparticles with diameter of 10-50 nm is formed, see Fig. 1c. The morphology of gold nanoparticles synthesized on the surface of this layer (Fig. 1d) significantly differs from morphology of gold nanoparticles obtained on the bare ITO electrode, the surface of $\text{Au}_x\text{SnO}_2(n3)\text{-Au}(n8)$ sample being covered with aggregated nanoparticles.

These aggregates of gold nanoparticles, which we can call «clusters», are 100-400 nm in diameter. As seen in histograms of particle size distribution of Fig. 2b, the diameter of the majority of nanoparticles does not exceed 20 nm in this case.

Investigation of the synthesized samples by UV-vis absorbance spectroscopy (Fig. 3) confirms the above results. UV-vis spectrum of Au(n8) sample shows a peak at 540 nm corresponding to the surface plasmon resonance (SPR) of gold nanoparticles with a diameter of 30-60 nm [65]. The spectrum of $\text{Au}_x\text{SnO}_2(n3)\text{-Au}(n8)$ sample demonstrates the SPR peak situated at a lower wavelength (535 nm) indicating the presence of smaller nanoparticles than in Au(n8) sample. Furthermore, a broad absorption band is observed at 985 nm which can be attributed to the absorbance of clusters of gold nanoparticles according to [66]. It should be noted that no shifting of SPR peaks is observed during the heating of the samples confirming the stability of the synthesized nanoparticles' sizes.

Significant changes in the morphology of Au(n8) and $\text{Au}_x\text{SnO}_2(n3)\text{-Au}(n8)$ samples can be explained by the presence of the preliminary synthesized $\text{Au}_x\text{SnO}_2 \cdot n\text{H}_2\text{O}$ layer, see Fig. 4. In case of the "a" route in Fig. 4, first cycle of SILD treatment of the

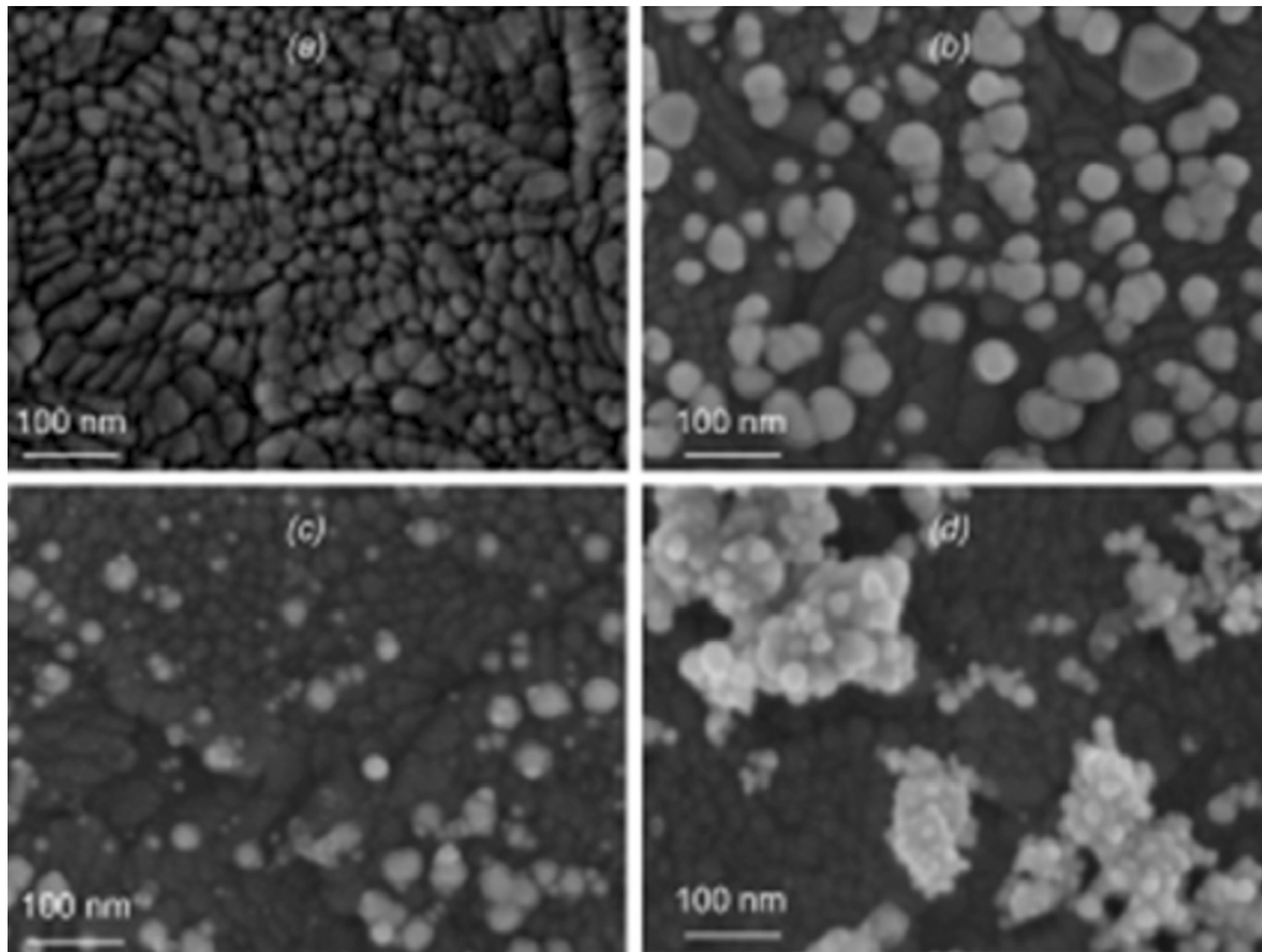


Fig. 1. SEM images of the ITO films modified by gold nanoparticles deposited by SILD method: (a) – initial sample (b) – Au(n8); (c) – $\text{Au}_x\text{SnO}_2(\text{n}3)$, (d) – $\text{Au}_x\text{SnO}_2(\text{n}3)\text{-Au}(\text{n}8)$.

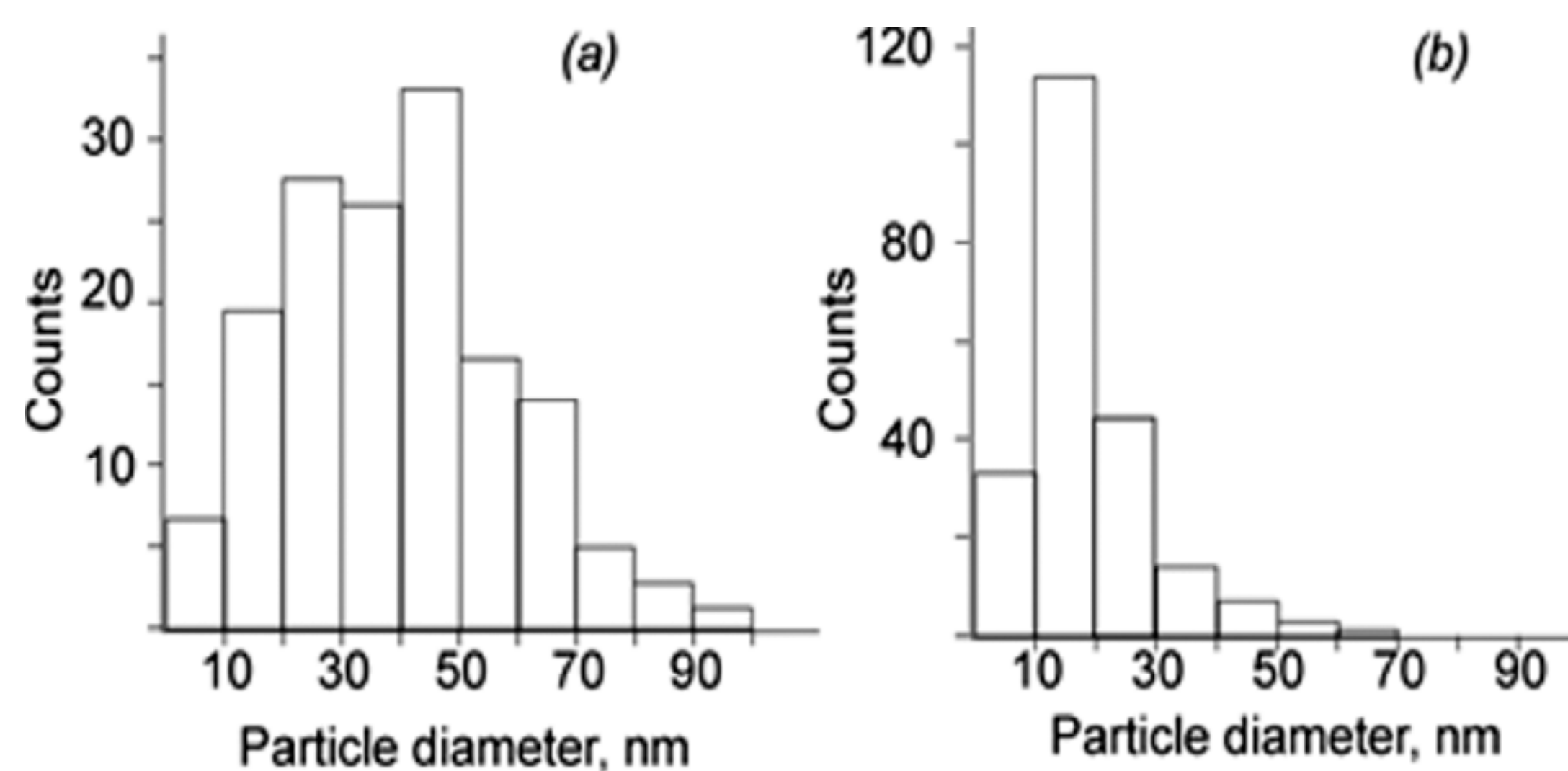


Fig. 2. Histogram of size distribution of gold nanoparticles on the surface of ITO substrate: (a) – Au(n8); (b) – $\text{Au}_x\text{SnO}_2(\text{n}3)\text{-Au}(\text{n}8)$.

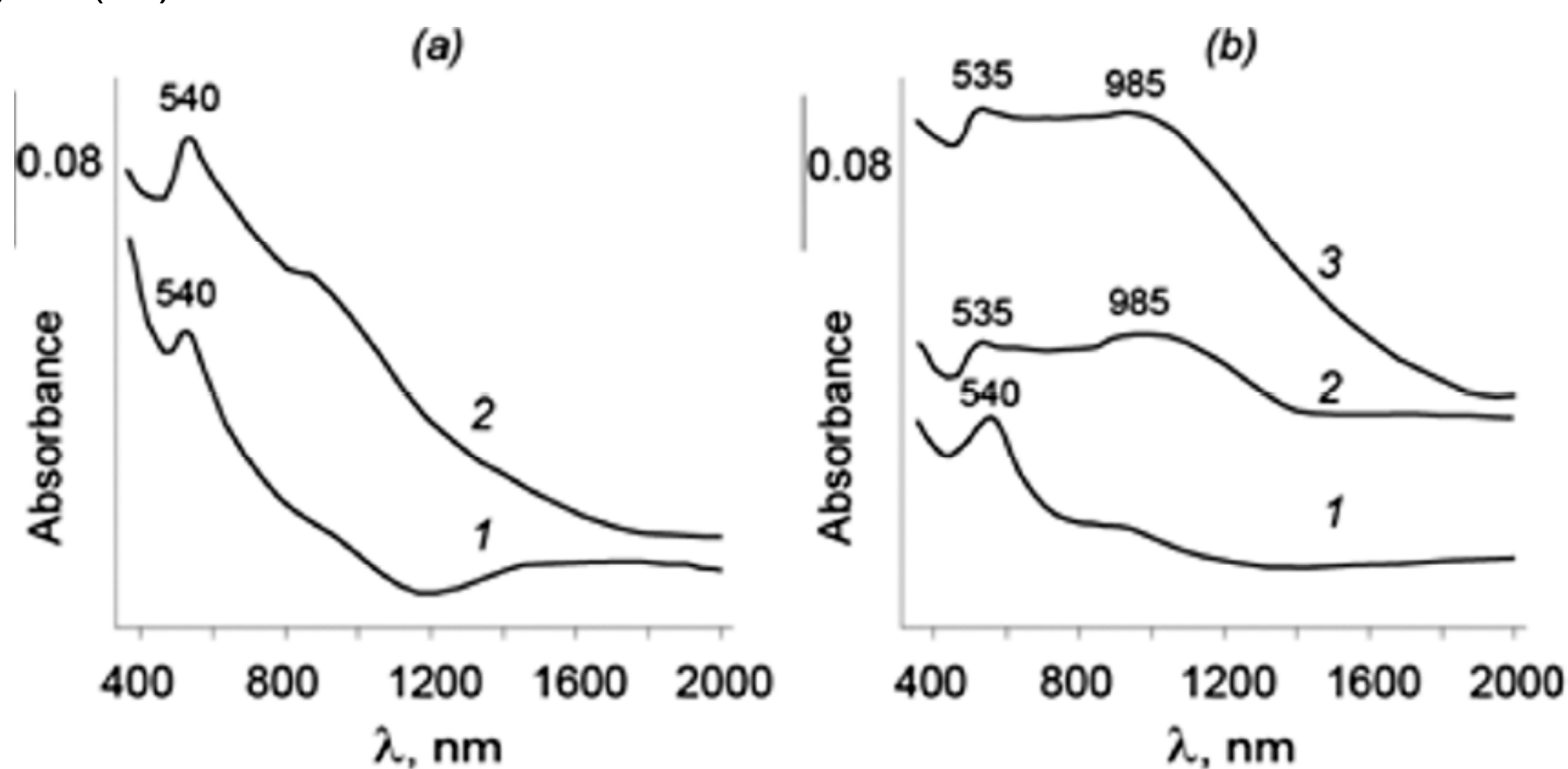


Fig. 3. UV–vis absorption spectra of gold nanoparticles on the surface of ITO substrate: (a) – Au(n8) before (1) and after (2) thermal treatment; (b) – $\text{Au}_x\text{SnO}_2(\text{n}3)$ (1), $\text{Au}_x\text{SnO}_2(\text{n}3)\text{-Au}(\text{n}8)$ before (2) and after (3) calcination.

surface results in the synthesis of gold nanoparticles at the active sites of the ITO surface, which has a polycrystalline structure. In agreement with [63], the

increase of the particles' size is observed during subsequent SILD cycles. If $\text{Au}_x\text{SnO}_2 \cdot n\text{H}_2\text{O}$ layer is pre-synthesized (the “b” route in Fig. 4), the reagents

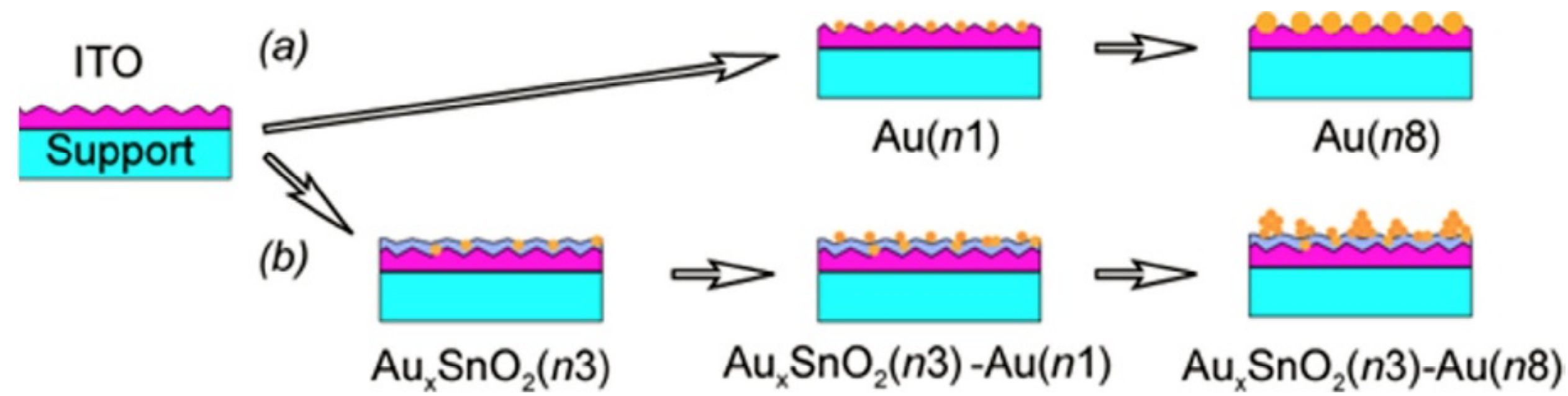


Fig. 4. Model of the formation of gold nanoparticles on the surface of ITO films during the SILD process.

are then adsorbed on the surface of amorphous $\text{SnO}_2 \cdot n\text{H}_2\text{O}$ layer and on the surface of gold nanoparticles included in this layer. We believe that amorphous structure of $\text{SnO}_2 \cdot n\text{H}_2\text{O}$ layer provides more uniform distribution of adsorbed ions and smaller size of the synthesized nanoparticles. Gold nanoparticles from the underlayer probably serve as centers for clusters formation. The effect of smaller gold nanoparticles migration during the heating of the sample in the air should also be taken into account.

Fig. 5 depicts the results of electrochemical study of the obtained electrodes. Recorded voltammograms demonstrate that the electrode modified with gold nanoparticles has larger effective surface area than flat gold electrode or unmodified ITO-electrode. According to the formula presented elsewhere the values of effective surface area were found to be $0.178 \pm 0.013 \text{ cm}^2$ for the flat gold electrode and $0.931 \pm 0.075 \text{ cm}^2$ for the modified ITO electrode ($\text{Au}_x\text{SnO}_2(n3)\text{-Au}(n8)$ sample). Obviously, this increase in the specific surface area is caused by the presence of a large quantity of gold nanoparticles and by the formation of 3D aggregates of these particles. In addition, the $\text{Au}_x\text{SnO}_2 \cdot n\text{H}_2\text{O}$ underlayer provides ohmic contact and relatively good adhesion of gold nanoparticles to the electrode surface. Positions of Au^0 oxidation peak (1.2 V) and Au^+ reduction peak (0.9 V) are also important. Compared to gold flat electrode, these peaks are shifted by 0.68 V and 0.7 V, respectively. These

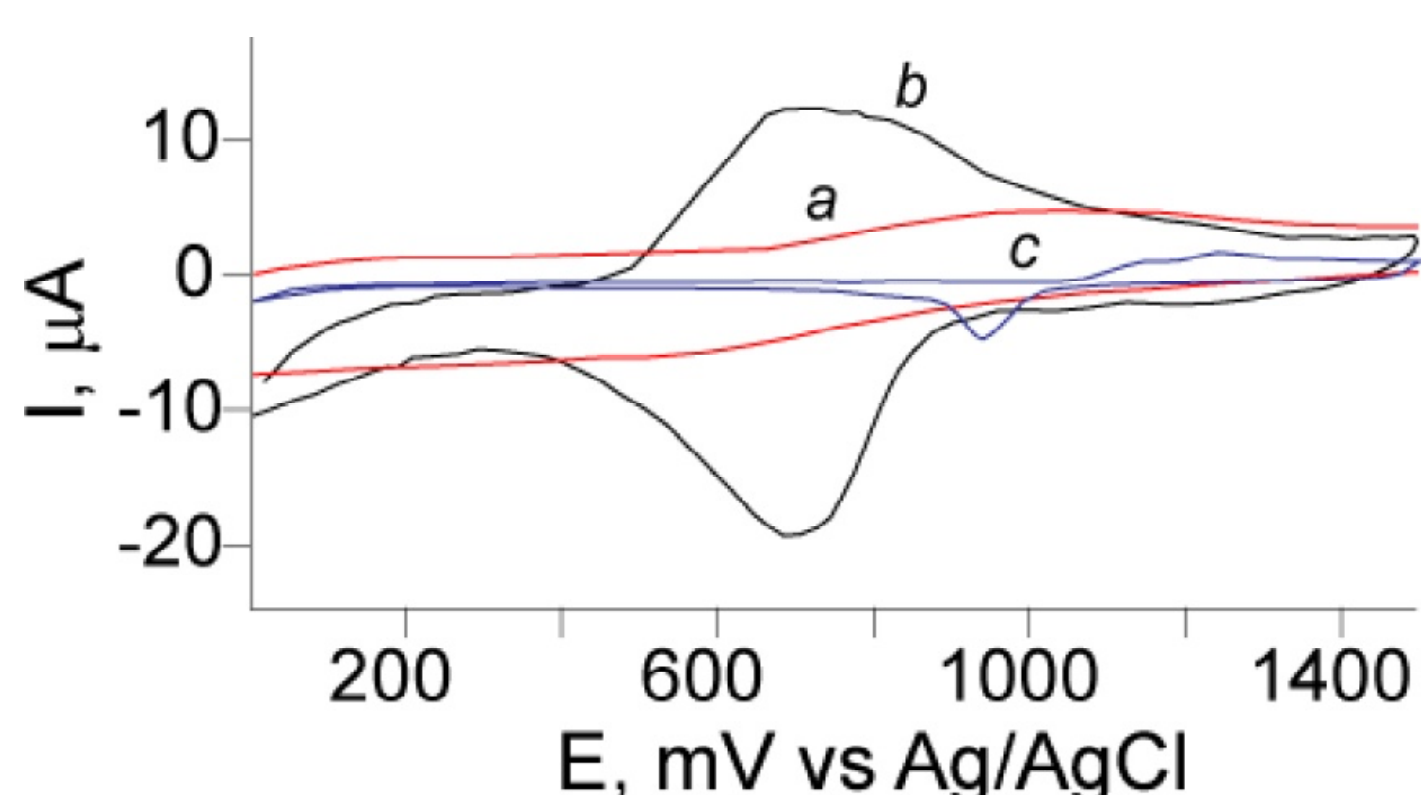


Fig. 5. Cyclic voltammograms in 0.1 M sulfuric acid recorded with: (a) – ITO-electrode; (b) – $\text{Au}_x\text{SnO}_2(n3)\text{-Au}(n8)$ on the ITO surface, (c) – flat gold electrode.

data indicate the high electrocatalytic activity of the synthesized gold nanoparticles. Similarly to [67], the observed effect of electrocatalysis can be explained by the presence of a large number of Au atoms directly on the surface of gold nanoparticles, including the surface of planes (100) or (110) of their crystalline structure [68].

6. CONCLUSION

Conducted analysis suggests that the immobilization of gold nanoparticles on inorganic surface is not a trivial task and its solution requires a search for new approaches to the formation of AuNPs with required size and shape. The SILD method of synthesis of AuNPs is suitable to solve certain practical problems of sensor design.

ITO electrode surface treatment by SILD method in HAuCl_4 and NaBH_4 solutions results in nanoparticles formation. Preliminary SILD synthesis of $\text{Au}_x\text{SnO}_2 \cdot n\text{H}_2\text{O}$ layer leads to significant changes in the morphology of subsequently synthesized gold nanoparticles. Samples obtained under these conditions are characterized by a significantly smaller gold nanoparticles size (within 10-20 nm in diameter) and their higher concentration per surface unit. The synthesized gold nanoparticles exhibit electrocatalytic properties which make the modified electrode very attractive as a base for biosensor fabrication including screen-printed electrodes technology [69]. The shift of gold dissolution potential in sulfuric acid proved the catalytic activity of gold nanoparticles obtained by SILD method. The proposed electrode modification technique allowed us to increase the effective surface area of the electrode and therefore improve the analytical performance of the electrocatalytic sensor.

ACKNOWLEDGMENTS

The authors acknowledge the financial support of the SPbSU (grant No 12.38.259.2014), RFBR (grant No 15-03-08045). We are grateful to the Nanotechnology Center of St. Petersburg State University for SEM studies of our samples.

REFERENCES

- [1] M. Faraday // *Phil. Trans. of the Royal Society of London* **147** (1857) 145.
- [2] G. Li and R.C. Jin // *Nanotechnol. Rev.* **2** (2013) 529.
- [3] K. Saha, S. Agasti, C. Kim, X. Li and V.M. Rotello // *Chem. Rev.* **112** (2012) 2739.
- [4] J.M. Pingarron, P. Yanez-Sedeno and A. Gonzalez-Cortes // *Electrochim. Acta* **53** (2008) 5848.
- [5] I. Pantic and L. Markovic // *Rev. Adv. Mater. Sci.* **29** (2011) 126.
- [6] A. Kumar, X. Zhang and X.J. Liang // *Biotechnol. Adv.* **31** (2013) 593.
- [7] S. Suresh and P. Mathan // *Rev. Adv. Mater. Sci.* **36** (2014) 112.
- [8] D.X. Li, Q. He and J.B. Li. // *Adv. Colloid Interface Sci.* **149** (2009) 28.
- [9] S. Choi, A. Tripathi and D. Singh // *J. Biomed. Nanotechnol.* **10** (2014) 3162.
- [10] M. Grzelczak, J. Perez-Juste, P. Mulvaney and L.M. Liz-Marzan // *Chem. Soc. Rev.* **37** (2008) 1783.
- [11] N. Li, P. Zhao and D. Astruc // *Angew. Chem. Int. Edit.* **53** (2014) 1756.
- [12] N. Khlebtsov and L. Dykman // *Chem. Soc. Rev.* **40** (2011) 1647.
- [13] D. Philip // *Spectrochim Acta A* **77** (2010) 807.
- [14] F. Wu and Q. Yang // *Nano Res.* **4** (2011) 861.
- [15] M. Brust, M. Walker, D. Bethell, D.J. Schiffrin and R. Whyman // *J. Chem. Soc., Chem. Commun.* **7** (1994) 801.
- [16] M. Bechelany, X. Maeder, J. Riesterer, J. Hankache, D. Lerose, S. Christiansen, J. Michler and L.M. Philippe // *Crystal Growth Des.* **10** (2010) 587.
- [17] J.P. Sylvestre, S. Poulin, A.V. Kabashin, E. Sacher, M. Meunier and J.H.T. Luong // *J. Phys. Chem. B* **108** (2004) 16864.
- [18] T.K. Sau and C.J. Murphy // *Langmuir* **21** (2005) 2923.
- [19] M.A. Bratescu, S.-P. Cho, O. Takai and N. Saito // *J. Phys. Chem. C* **115** (2011) 24569.
- [20] L. Xu, W. Ma, L. Wang, C. Xu, H. Kuang and N.A. Kotov // *Chem. Soc. Rev.* **42** (2013) 3114.
- [21] C. Bai and M. Liu // *Nano Today* **7** (2012) 258.
- [22] J.C. Fierro-Gonzalez and B.C. Gates // *Chem. Soc. Rev.* **37** (2008) 2127.
- [23] S. Guo and E. Wang // *Anal. Chim. Acta* **598** (2007) 181.
- [24] K. Nikolaev, S. Ermakov, Yu. Ermolenko, E. Averyaskina, A. Offenhäusser, and Yu. Mourzina // *Bioelectrochemistry* **105** (2015) 34.
- [25] R. Palgrave and I. Parkin // *Gold Bull.* **41** (2008) 66.
- [26] E. Ertorer, J.C. Avery, L.C. Pavelka and S. Mittler // *Chem. Vap. Dep.* **19** (2013) 338.
- [27] V.G. Pol, A. Gedanken and J. Calderon-Moreno // *Chem. Mat.* **15** (2003) 1111.
- [28] K.B. Blodgett and I. Langmuir // *Phys. Rev.* **51** (1937) 964.
- [29] J. Turkevich, P. C. Stevenson and J. Hiller. // *Discuss. Faraday Soc.* **11** (1951) 55.
- [30] G. Chen, M. Takezawa, N. Kawazoe and T. Tateishi // *Open Biotechnol. J.* **2** (2008) 152.
- [31] W. Patungwasa and J.H. Hodak // *Mat. Chem. Phys.* **108** (2008) 45.
- [32] R. Zanella, S. Giorgio, C.R. Henry and C. Louis // *J. Phys. Chem. B* **106** (2002) 7634.
- [33] P. Sangeetha and Y.-W. Chen // *Int. J. Hydrogen Energy* **34** (2009) 7342.
- [34] Y.-W. Chen, D.-S. Lee and H.-J. Chen // *Int. J. Hydrogen Energy* **37** (2012) 15140.
- [35] A. Primo, A. Corma and H. Garcia // *Phys. Chem. Chem. Phys.* **13** (2011) 886.
- [36] K. Ariga, J.P. Hill and Q. Ji // *Phys. Chem. Chem. Phys.* **9** (2007) 2319.
- [37] J.P. Chapel and J.F. Berret // *Curr. Opin. Colloid In.* **17** (2012) 97.
- [38] R.K. Iler // *J. Colloid Interf. Sci.* **21** (1966) 569.
- [39] Y. Lvov, K. Ariga, I. Ichinose and T. Kunitake // *J. Am. Chem. Soc.* **117** (1995) 6117.
- [40] G. Decher and J. D. Hong // *Makromol. Chem., Macromol. Symp.*, **46** (1991) 321.
- [41] T.R. Farhat and J.B. Schlenoff // *Langmuir* **17** (2001) 1184.
- [42] X. Zhang, H. Chen and H. Zhang // *Chem. Comm.* (2007) 1395.
- [43] F. Kurniawan, V. Tsakova and V.M. Mirsky // *Electroanal.* **18** (2006) 1937.
- [44] Y. Sun, F. Yan, W. Yang and C. Sun // *Biomaterials* **27** (2006) 4042.
- [45] W. Yang, J. Wang, S. Zhao, Y. Sun and C. Sun // *Electrochem. Commun.* **8** (2006) 665.

- [46] B.-Y. Wu, S.-H. Hou, F. Yin, Z.-X. Zhao, Y.-Y. Wang, X.-S. Wang and Q. Chen // *Biosens. Bioelectron.* **22** (2007) 2854.
- [47] T.-R. Kuo, D.-Y. Wang, Y.-C. Chiu, Y.-C. Yeh, W.-T. Chen, C.-H. Chen, C.-W. Chen, H.-C. Chang, C.-C. Hu and C.-C. Chen // *Anal. Chim. Acta* **809** (2014) 97.
- [48] C. Ou, R. Yuan, Y. Chai, M. Tang, R. Chai and X. He // *Anal. Chim. Acta* **603** (2007) 205.
- [49] P. Wang, Y. Li, X. Huang and L. Wang // *Talanta* **73** (2007) 431.
- [50] B.-Y. Wu, S.-H. Hou, F. Yin, J. Li, Z.-X. Zhao, J.-D. Huang and Q. Chen // *Biosens. Bioelectron.* **22** (2007) 838.
- [51] S. Guo, L. Xu, B. Xu, Z. Sun and L. Wang // *Analyst* **140** (2015) 820.
- [52] Cai, X. Gao, L. Wang, Q. Wu and X. Lin // *Sensor Actuat. B-Chem.* **181** (2013) 575.
- [53] L.B. Gulina, V.P. Tolstoy and E.V. Tolstobrov // *Russ. J. Appl. Chem.* **83** (2010) 1525.
- [54] L.B. Gulina and V.P. Tolstoy // *Thin Solid Films* **440** (2003) 74.
- [55] V.P. Tolstoy // *Russ. Chem. Rev.* **75** (2006) 161.
- [56] V.P. Tolstoy // *Thin Solid Films* **307** (1997) 10.
- [57] G. Korotcenkov, B.K. Cho, V. Brinzari, L.B. Gulina and V.P. Tolstoy // *Ferroelectrics* **459** (2014) 46.
- [58] G. Korotcenkov, B.K. Cho, L.B. Gulina and V.P. Tolstoy // *Sensor Actuat. B-Chem.* **166-167** (2012) 402.
- [59] G. Korotcenkov, B.K. Cho, L.B. Gulina and V.P. Tolstoy // *WASET* **81** (2011) 199.
- [60] G. Korotcenkov, V. Tolstoy, J. Schwank and I. Boris // *J. Phys.: Conf. Ser.* **15** (2005) 45.
- [61] G. Korotcenkov, L. B. Gulina, B. K. Cho, S.H. Han and V. P. Tolstoy // *Mat. Chem. Phys.* **128** (2011) 433.
- [62] G. Korotcenkov, B.K. Cho, L. Gulina and V. Tolstoy // *Sensor Actuat. B-Chem.* **141** (2009) 610.
- [63] G. Korotcenkov, L.B. Gulina, B. Cho, V. Brinzari and V.P. Tolstoy // *Pure Appl. Chem.* **86** (2014) 801.
- [64] G. Korotcenkov, V. Brinzari and B.K. Cho // *Mater. Lett.* **147** (2015) 101.
- [65] N.G. Khlebtsov and L.A. Dykman // *J. Quant. Spectrosc. Radiat. Transf.* **111** (2010) 1.
- [66] E. Hutter and J.H. Fendler // *Adv. Mater.* **16** (2004) 1685.
- [67] K.G. Nikolaev, S.S. Ermakov, A. Offenhäusser and Y. Mourzina // *Mendeleev Commun.* **24** (2014) 145.
- [68] A. Hamelin // *J. Electroanal. Chem.* **407** (1996) 1.
- [69] D. Timofeeva, Yu. Tsapko, S. Ermakov // *J. Electroanal. Chem.* **660** (2011) 195.